Correction for Chemical Shift Artifacts in Magnetic Resonance Electrical Impedance Tomography

M. J. Hamamura[1], O. Nalcioglu[1], and L. T. Muftuler[1]

[1]Tu & Yuen Center for Functional Onco-Imaging, University of California, Irvine, CA, United States

Introduction

Several *ex vivo* studies have reported that the electrical impedance of malignancies is lower than healthy tissues and benign formations [Malich *et al*, Eur Radiol 10:1555-61 (2000)]. Therefore, *in vivo* conductivity imaging may have potential applications in tumor diagnosis. Magnetic resonance electrical impedance tomography (MREIT) is an emerging, non-invasive conductivity imaging modality, in which electrical currents are injected into an object and the resulting magnetic flux density distribution is measured using MRI; these MRI measurements are then used to reconstruct the conductivity distribution within the object.

Only a very limited number of *in vivo* MREIT studies have been reported. Obstacles limiting *in vivo* application include restrictions on the maximum (safe) level of injected currents, motion artifacts, and chemical shift artifacts. With chemical shift artifacts, the location of fat tissues appear shifted along the readout direction, which results in a distortion of the phase maps utilized in MREIT. Use of low readout bandwidths for improving the SNR when using lower injected current levels further magnifies these artifacts.

In this study, we corrected for chemical shift artifacts in order to generate accurate phase maps for use in MREIT. The standard 3-point Dixon technique [Glover *et al*, Mag Res Med 18:371-383 (1991)] was appropriately modified to generate separated water and fat phase maps. The fat images were then corrected for chemical shift and recombine with the water images to generate the total corrected phase maps. These phase maps were then used to reconstruction the conductivity distribution.

Methods

For the test phantom, a hollow acrylic disk with an inner diameter of 7 cm and thickness of 2 cm was filled with 2% agarose and 10 mM $CuSO_4$. Within this disk, a smaller cylindrical shell of 12mm diameter was placed slightly off-center and filled with vegetable oil (Fig. 1). The plane of the phantom was placed perpendicular to the main static MRI field (z-direction). Three copper electrodes each 2 mm wide were placed equidistant along the inner acrylic wall and used to inject currents into the interior region.

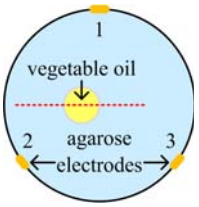

Fig. 1. *Phantom*

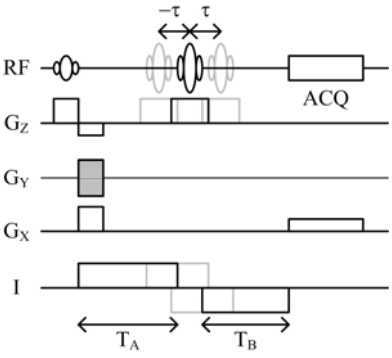

Fig. 2. *MREIT/Dixon pulse sequence*

Data was collected using a 4 T MRI system. A 2 mA bipolar current pulse was injected into the phantom and the resulting z-component magnetic flux density distribution B_Z was measured using a modified (asymmetric) spin-echo pulse sequence [Scott *et al*, IEEE TMI 10:362-374 (1991)] as diagramed in Fig. 2. Three data sets (S_{0A},S_{1A},S_{-1A}) were acquired with the position of the 180 degree pulse shifted by 0, τ, and -τ respectively. The value of τ (420 μs) was selected such that the water (agarose) and fat (vegetable oil) signals were at opposite phases. A 4th data set (S_{0B}) was acquired with no echo shift and with the polarity of the injected current waveform reversed. Common scan parameters were: TR = 500 ms, TE = 50 ms, T_A+T_B = Tc = 44 ms, BW = 20 kHz, FOV = 10 cm, matrix = 128 x 128, slice thickness = 5 cm, NEX = 2.

From the 4 data sets, the separated (complex) water ρ_1'' and fat ρ_2'' images were computed as outlined in Fig. 3, where additional variables are defined as: ρ_1 = water magnitude, ρ_2 = fat magnitude, ψ = system phase contributions, γ = gyromagnetic ratio, ϕ = B_0 phase contribution, θ = switch angle. The separated fat/water B_Z maps were then determined from the argument of these images. The fat maps were corrected for chemical shift, then recombined with the water maps to generate the total corrected B_Z map. Two B_Z maps (B_{12}, B_{13}) were calculated using electrode pairs 1&2 and 1&3 respectively for current injection, and used simultaneously in the conductivity reconstruction. To reconstruct the conductivity distribution using the MRI measurements, the iterative sensitivity matrix method (SMM) with Tikhonov regularization was utilized, where the relationship between conductivity and magnetic flux density is linearized around an initial conductivity (i.e. uniform distribution) and formulated as a matrix equation [Birgul *et al*, Phys Med Biol 51:5035-5049 (2006)].

$$S_{0A} = (\rho_1 + \rho_2)\, e^{i\psi} e^{i\gamma Bz\, Tc}$$
$$S_{1A} = (\rho_1 - \rho_2)\, e^{i\psi} e^{i\phi} e^{i\gamma Bz\, Tc}$$
$$S_{-1A} = (\rho_1 - \rho_2)\, e^{i\psi} e^{-i\phi} e^{i\gamma Bz\, Tc}$$
$$S_{0B} = (\rho_1 + \rho_2)\, e^{i\psi} e^{-i\gamma Bz\, Tc}$$

$$h_A \equiv e^{i\psi} e^{i\gamma Bz\, Tc},\ h_B \equiv e^{i\psi} e^{-i\gamma Bz\, Tc}$$

$$S_{-1A}' \equiv S_{-1A}\, h_A^* = (\rho_1 - \rho_2)\, e^{-i\phi},\ \phi = \arg(S_{1A}\, S_{-1A}^*)/2$$
$$\theta = \arg(S_{-1A}'\, e^{-i\phi})$$

$$S_{0A}'' \equiv S_{0A}\, h_B^* = (\rho_1 + \rho_2)\, e^{2i\gamma Bz\, Tc}$$
$$S_{1A}'' \equiv S_{1A}\, h_B^* = (\rho_1 - \rho_2)\, e^{i\phi} e^{2i\gamma Bz\, Tc}$$
$$S_{-1A}'' \equiv S_{-1A}\, h_B^* = (\rho_1 - \rho_2)\, e^{-i\phi} e^{2i\gamma Bz\, Tc}$$

$$\rho_1'' = \rho_1\, e^{2i\gamma Bz\, Tc} = (S_{0A}'' + \cos\theta\,(S_{1A}''\, S_{-1A}''))^{1/2})/2$$
$$\rho_2'' = \rho_2\, e^{2i\gamma Bz\, Tc} = (S_{0A}'' - \cos\theta\,(S_{1A}''\, S_{-1A}''))^{1/2})/2$$

Fig. 3. *Modified 3-point Dixon technique*

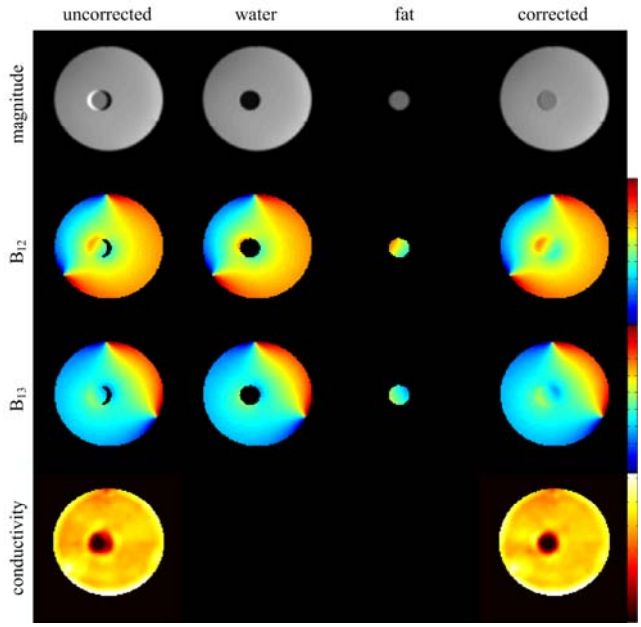

Fig 4. *Uncorrected, water, fat, and corrected images*

Results

The uncorrected, separated fat/water, and corrected images are shown in Fig. 4. Separation of the water and fat images was accomplished using the previously outlined modified 3-point Dixon technique. Relative conductivities were reconstructed from the B_Z maps using 10 iterations of the SMM. The profile of the conductivity reconstruction across the red dotted line of Fig. 1 is shown in Fig. 5.

Discussion

Inspection of Fig. 4 reveals that chemical shift artifacts both distort the B_Z maps and leave a region of signal void. Consequentially, the resulting conductivity reconstruction suffers, as also seen in Fig. 5. Through the use of a modified 3-point Dixon algorithm, B_Z maps free of chemical shift artifacts were generated, resulting in improved conductivity reconstruction. In addition to this algorithm, more recently developed fat/water separation techniques may potentially be modified for use in MREIT and could offer improved performance.

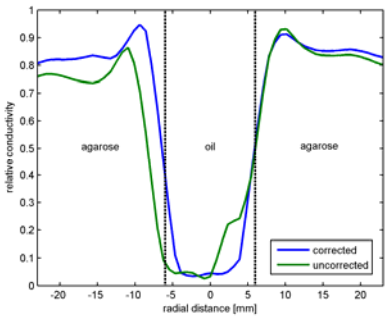

Fig. 5. *Conductivity profile*

The results of this study demonstrate that chemical shift artifacts can adversely affect the accuracy of MREIT, and that appropriate application of a modified 3-point Dixon technique can alleviate this problem. Correction of chemical shift artifacts in MREIT will be crucial in future *in vivo* studies, particularly when imaging regions with large fat content such as the breast.

This research is supported in part by NIH R01 CA114210.